NeuroImage 210 (2020) 116578

Contents lists available at ScienceDirect

NeuroImage

journal homepage: www.elsevier.com/locate/neuroimage

Community structure of the creative brain at rest

Yoed N. Kenett [a,*,1], Richard F. Betzel [b,c,d,e,1], Roger E. Beaty [f]

[a] Department of Psychology, University of Pennsylvania, Philadelphia, PA, 19104, USA
[b] Department of Psychological and Brain Sciences, Indiana University, Bloomington, IN, 47405, USA
[c] Cognitive Science Program, Indiana University, Bloomington, IN, 47405, USA
[d] Program in Neuroscience, Indiana University, Bloomington, IN, 47405, USA
[e] Network Science Institute, Indiana University, Bloomington, IN, 47405, USA
[f] Department of Psychology, Pennsylvania State University, University Park, PA, 16801, USA

ARTICLE INFO

Keywords:
Creativity
Resting-state
Community structure
Divergent thinking
Default mode network

ABSTRACT

Recent studies have provided insight into inter-individual differences in creative thinking, focusing on characterizations of distributed large-scale brain networks both at the local level of regions and their pairwise interactions and at the global level of the brain as a whole. However, it remains unclear how creative thinking relates to mesoscale network features, e.g. community and hub organization. We applied a data-driven approach to examine community and hub structure in resting-state functional imaging data from a large sample of participants, and how they relate to individual differences in creative thinking. First, we computed for every participant the co-assignment probability of brain regions to the same community. We found that greater capacity for creative thinking was related to increased and decreased co-assignment of medial-temporal and subcortical regions to the same community, respectively, suggesting that creative capacity may be reflected in inter-individual differences in the meso-scale organization of brain networks. We then used participant-specific communities to identify network hubs—nodes whose connections form bridges across the boundaries of different communities—quantified based on their participation coefficients. We found that increased hubness of DMN and medial-temporal regions were positively and negatively related with creative ability, respectively. These findings suggest that creative capacity may be reflected in inter-individual differences in community interactions of DMN and medial-temporal structures. Collectively, these results demonstrate the fruitfulness of investigating mesoscale brain network features in relation to creative thinking.

1. Introduction

Neurocognitive research on brain structure and dynamics related to creative thinking is increasingly growing, with an established society for the Neuroscience of Creativity (https://tsfnc.org/), several systematic reviews, edited books, and special issues dedicated to the topic (e.g., Abraham, 2018; Beaty et al., 2016; Beaty et al., 2019; Benedek and Fink, 2019; Benedek et al., 2018; Gonen-Yaacovi et al., 2013; Shen et al., 2017). These endeavors have greatly benefited from network neuroscience methodologies (Medaglia et al., 2015), applying graph theoretical methods to represent and study the brain as a complex system. Network neuroscience research of creativity has begun to reveal the network structure and dynamics that underpin the complex mechanisms of the creative brain (Beaty et al., 2019). Such studies have, for example, identified unique functional connectivity patterns that predict individual differences in creative ability (Beaty et al., 2018; Gao et al., 2017; Li et al., 2017; Sun et al., 2019; Takeuchi et al., 2012, 2017; Wei et al., 2014), investigated how brain networks interact during divergent thinking (Beaty et al., 2015; Beaty et al., 2017; Benedek et al., 2016; Green et al., 2015; Shi et al., 2018; Vartanian et al., 2018), and examined how white matter connectivity patterns constrain neural dynamics in relation to creative thinking (Kenett et al., 2018; Ryman et al., 2014).

Several studies have examined how functional connectivity patterns in resting-state (RS) fMRI data relate to creative performance (Beaty et al., 2014; Fink et al., 2018; Shi et al., 2018; Sun et al., 2019; Zhu et al., 2017). Functional connectivity of RS-fMRI measures synchronized patterns of spontaneous brain activation during rest (Fox and Raichle, 2007). Such studies typically collect RS fMRI data, compute network

* Corresponding author. University of Pennsylvania, Department of Psychology, Philadelphia, PA, 19104, USA.
E-mail address: yoedk@sas.upenn.edu (Y.N. Kenett).
[1] Authors contributed equally to the manuscript.

https://doi.org/10.1016/j.neuroimage.2020.116578
Received 16 July 2019; Received in revised form 14 November 2019; Accepted 19 January 2020
Available online 23 January 2020

connectivity via Pearson's correlations, and then associate features of these networks with participants' performances on a divergent thinking task. Divergent thinking (DT) tasks measure a person's ability to generate solutions to open-ended problems, such as inventing new uses for objects (Acar and Runco, 2019; Runco and Acar, 2012). DT tasks are considered to provide a reliable index of general creative ability (Acar and Runco, 2019; Runco and Acar, 2012). RS fMRI studies have shown that higher coupling between the default mode network (DMN) and the executive control network (ECN) in the "resting brain" is correlated with higher DT performance (Beaty et al., 2014; Zhu et al., 2017). A recent study found that DMN-ECN coupling at rest predicts the strength of the connections between these two networks during performance on a DT task (Shi et al., 2018), highlighting the utility of analyzing RS data in relation to creative performance. Finally, Fink et al. (2018) have recently shown that training in DT leads to changes in the connectivity patterns of several brain networks in RS data, further demonstrating a correspondence between RS and task-state brain networks relevant to creative thought. All of these studies focus on features of structural and functional brain networks at the local scale of brain regions and their connections.

Many studies have investigated network architecture and its relationship with cognition at the local scale of individual nodes and edges. For example, by assessing the extent to which the weight of a functional connection is correlated with performance on a task. Alternatively, many studies have addressed similar questions at the global scale of the network as a whole. For example, by assessing the extent to which network measures like efficiency (Latora and Marchiori, 2001) vary with performance. However, brain function and dynamics are also shaped by organizational properties of clusters or modules (i.e., at the meso-scale; Fortunato, 2010; Meunier et al., 2010; Sporns and Betzel, 2016). In the current study, we extended network neuroscientific research on creativity by examining how individual differences in community organization of resting-state functional connectivity networks relate to individual differences in creative behavior.

Situated between the local and global network level extremes is a rich meso-scale that emphasizes subgraphs comprised of groups of nodes and edges (Betzel and Bassett, 2017). In practice, these subgraphs are referred to as modules or communities and defined as groups of nodes that are more strongly connected to other nodes in the same community than to nodes in different communities (Betzel et al., 2017, 2018, 2019; Gallen and D'Esposito, 2019; Meunier et al., 2010; Power et al., 2011), Because the brain regions that make up these communities exhibit similar connectivity patterns and are mutually connected to one another, communities are usually interpreted as subtending similar brain and cognitive function (Bertolero et al., 2015; Gallen and D'Esposito, 2019). By characterizing the variability of community structure across individuals or between clinical populations, recent studies seek a deeper understanding of neuropsychiatric disorders, development and aging, and diverse cognitive processes (Cole et al., 2014; de Haan et al., 2012; Gu et al., 2015). However, to date such potential differences in RS community structure in relation to creative ability have not been explored.

While a network's community structure describes relationships among groups of nodes, it also can be used to define and characterize the functional roles of individual nodes in the network (Crossley et al., 2014; Power et al., 2013). Previous studies have highlighted the importance of hubs in brain structure and function, and their role in realizing cognitive functions (Sporns and Betzel, 2016; van den Heuvel and Sporns, 2013). The participation coefficient (PC; Guimera and Amaral, 2005), for instance, is a measurement computed based on a network's community structure and the distribution of each node's connections across communities (Fig. 1). Intuitively, the connections of nodes with high PC are distributed evenly across communities, while the connections of nodes with low PC are concentrated within a small number of communities. In the context of neuroscience, PC is one of many indices that contribute to define a brain region's "hubness"; brain regions associated with larger values of PC, by definition, straddle the boundaries of communities, and are thought to reflect integration of information between communities (Bertolero et al., 2015; Bertolero et al., 2018).

In the current study, we explore meso-scale RS network features in relation to individual differences in creative thinking, as measured by DT. We also aimed to identify specific network hubs that influence meso-scale network communities in the highly creative resting brain. In line with previous findings on the importance of functional connectivity patterns across brain systems in predicting creative ability (Beaty et al., 2018), we expected to find patterns of community structure across participants—mainly ECN-DMN-SN—that related to individual differences in creativity. In line with previous findings on the role of the DMN in individual differences in creativity (Beaty et al., 2019), we expected to find greater PC in DMN regions is associated with individual differences in creative ability.

2. Methods and materials

2.1. Participants

The data was collected as part of a larger study on individual differences in creativity and imagination (Beaty et al., 2018). The total sample

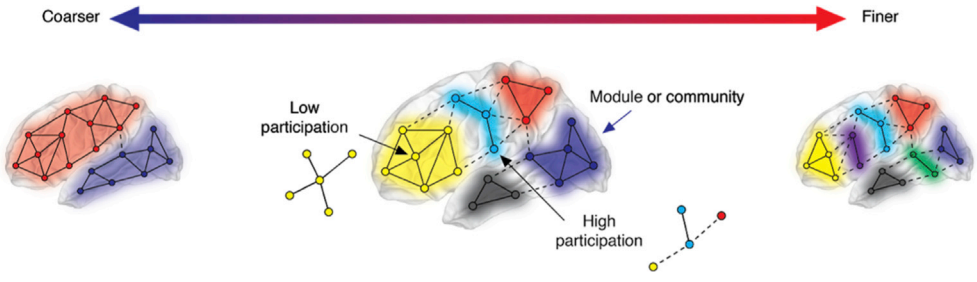

Fig. 1. Schematic illustration of network measures. In this study we use the concept of multi-scale modularity and the network measurement participation coefficient to investigate network-level correlates of creativity. In this figure, we illustrate these concepts. Modules refer to groups of nodes that are strongly connected to other nodes in the same module but weakly connected to other modules. Here, we identify modules by depicting all the nodes in the same module the same color. Importantly, modular structure can be defined at multiple scales or levels, encompassing coarse scales corresponding to divisions of the network into a few large modules to finer scales in which the network is partitioned into many small modules. Given a set of modules, the nodal measure "participation coefficient" can be used to identify nodes whose connections form bridges across different modules (high participation) or are concentrated within a small set of modules (low participation).

consisted of 163 participants recruited from the University of North Carolina at Greensboro (UNCG) and surrounding community (113 women, mean age = 22.50, SD = 5.79). All participants were right-handed with normal or corrected-to-normal vision, and reported no history of neurological disorder, cognitive disability, or medication that affects the central nervous system. The study was approved by the UNCG Institutional Review Board.

2.2. Materials

2.2.1. Assessment of creative thinking

Participants' creative ability was measured via a series of DT tasks, conducted during a separate task-based functional MRI scan as well as on a computer outside the scanner (see Beaty et al., 2018). Participants were presented with a series of common objects and were asked, for each object, to imagine a new and unusual use for it (Beaty et al., 2015). For the computer-based assessment, participants had 2 min to continuously generate alternate uses for two objects (i.e., box and rope) by typing their responses on a desktop computer. For the scanner-based assessment, participants had 12 s to think of a single alternate use for 23 other common objects, and 5 s to verbally report their response *via* an MRI compatible microphone (Beaty et al., 2018; Benedek et al., 2019). Responses in both DT tasks (inside and outside the scanner) were rated for their creativity by four trained raters, using a 1 (*not at all creative*) to 5 (*very creative*) scale (Hass et al., 2018). Raters were instructed to consider uncommonness, remoteness, and cleverness when coding responses, but to provide a single holistic score for each response (Silvia et al., 2008). Raters exhibited good inter-rater reliability for both DT tasks that were conducted inside (averaged ICC = 0.78) and outside (averaged ICC = 0.72) the scanner.

Confirmatory factor analysis was used to model the creativity ratings of the DT tasks performed inside and outside the scanner (see Beaty et al., 2018). This approach has been widely used, particularly in creativity research with subjective creativity ratings (Silvia et al., 2008), to model error variance separately from true measurement variance, yielding a more robust and reliable assessment of underlying trait-level factors compared to averaging (Kline, 2015). Here we specified a higher-order latent variable model using Mplus 7.2 (Muthén and Muthén, 2012). The higher-order creativity factor was indicated by two lower-order latent factors: ratings of the DT task conducted inside the scanner and ratings of the DT task conducted outside the scanner (see Beaty et al., 2018 for more details on model specification). This latent model was used to compute latent DT scores for all participants. The distribution of participants latent DT score was normally distributed, mean DT score = 0, SD = 0.85, skewness = 0.254 (SI Fig. 1). Finally, participant's age did not correlate with their latent DT score, $r(162) = 0.08$, $p = 0.33$.

2.2.2. MRI data acquisition and preprocessing

Resting-state functional imaging data were acquired for 5 min as participants relaxed awake in the scanner with eyes closed. Whole-brain imaging was performed on a 3T Siemens Magnetom MRI system (Siemens Medical Systems, Erlangen, Germany) using a 16-channel head coil. BOLD-sensitive T2*-weighted functional images were acquired using a single shot gradient-echo EPI pulse sequence (TR = 2000 ms, TE = 30 ms, flip angle = 78°, 32 axial slices, 3.5 × 3.5 × 4.0 mm, distance factor 0%, FoV = 192 × 192 mm, interleaved slice ordering) and corrected online for head motion. A high resolution T1 scan was acquired for anatomical normalization.

Functional volumes were preprocessed using the CONN toolbox (http://www.nitrc.org/projects/conn; Whitfield-Gabrieli and Nieto-Castanon, 2012) in MATLAB. For each participant, CONN implemented CompCor, a method for identifying principal components associated with segmented white matter (WM) and cerebrospinal fluid (CSF). In a first-level analysis, CompCor components and first-order derivatives of motion were entered as confounds and regressed from the BOLD signal. Additional preprocessing steps—similar to those applied in Beaty et al. (2018)—included high-pass filtering, linear detrending, and regression of outlying functional volumes (>97th percentile in normative sample; global-signal z-value threshold = 5, participant-motion mm threshold = 0.09) identified using the artifact removal toolbox (ART; https://www.nitrc.org/projects/artifact_detect/).

2.2.3. Functional network construction

Whole-brain networks were computed for each participant using CONN. Consistent with past work (Beaty et al., 2018; Finn et al., 2015; Rosenberg et al., 2016), we used the Shen brain atlas, which consists of 268 brain regions of 2 mm dimensions and provides whole-brain coverage of the cerebral cortex, cerebellum, and brain stem (Shen et al., 2013). BOLD signal was extracted from each brain region, and Fisher-transformed Pearson correlations were computed between each pair of brain regions, resulting in a 268 × 268 brain region correlation matrix for each participant.

2.2.4. Community detection

Brain networks can be analyzed at multiple scales, from the level of individual nodes (local scale) to that of the network as a whole (global scale). Situated between these extremes is a meso-scale, which focuses on clusters of nodes and edges referred to as *modules* or *communities* (Sporns and Betzel, 2016). Typically, a network's community structure is unknown *a priori* and must be estimated algorithmically using community detection algorithms—data-driven heuristics for determining the number and identity of communities in a network. Though many community detection algorithms exist, among the most popular is modularity maximization (Newman and Girvan, 2004). Modularity maximization compares an observed pattern of connectivity with the pattern of connectivity expected under a null connectivity model and groups nodes into communities such that the total weight of within-module connections maximally exceeds that of the null model. This intuition is formalized by the modularity quality function:

$$Q = \sum_{ij} \left[A_{ij} - \gamma P_{ij}\right] \delta(\sigma_i \sigma_j)$$

In this expression A_{ij} and P_{ij} are the observed and expected weight of the connection between nodes i and j, and $\delta(x, y)$ is the Kronecker delta function, which returns a value of 1 when its arguments are equal and 0 others. Here, the inputs to the delta function are σ_i and σ_j, which represent the community assignments of nodes i and j. Effectively, the only elements that contribute to the above summation come from pairs of nodes assigned to the same community. Finally, γ is a structural resolution parameter, which scales the relative importance of the null connectivity model (Reichardt and Bornholdt, 2006). This parameter can be selectively tuned to different values, with smaller and larger values resulting in correspondingly larger and smaller communities.

Here, because the functional brain networks that we study are based on correlation matrices, we used the null connectivity model suggested by Bazzi et al. (2016) and set $P_{ij} = 1$ for all pairs of nodes. This particular null model treats the expected correlation between pairs of nodes as uniform and can be scaled according to the γ parameter. This particular model also addressed interpretational issues associated with other null models typically used for the analysis of correlation-based networks (Rubinov and Sporns, 2011). Also, because the correct number of communities was unknown ahead of time, we allowed the structural resolution parameter, γ, to vary over a range. Specifically, we examined 31 different values approximately logarithmically spaced over the interval 0 to 0.2 (corresponding to the 50th percentile of all positive functional connections aggregated across all participants). We did not analyze larger values, as they tended to result in partitions of the network into >100 communities.

Finally, community detection was performed separately for each of the 163 participants with usable fMRI data and creativity scores (Fig. 1). We optimized modularity using a generalization of the so-called

"Louvain" algorithm (Blondel et al., 2008), a greedy algorithm that, in benchmarks, has proven both accurate and fast. Specifically, we used the GenLouvain software package implemented in MATLAB (Jutla et al., 2011). Because the Louvain algorithm is non-deterministic, we performed 50 repetitions of the Louvain algorithm for each participant and value of γ.

2.2.5. Community co-assignment matrices

Due to the stochastic nature of the Louvain optimization algorithm and the fact that, in general, there exists a degeneracy of near-optimal partitions (Good et al., 2010), we elected to not focus on single point estimates of community structure, but to construct more continuous measures of nodes' community assignments. To this end, we computed the community co-assignment probability, C_{ij}, for every pair of nodes. Given R partitions of a network into (potentially) different communities, the co-assignment probability of nodes i and j is equal to the fraction of all partitions in which those nodes are assigned to the same community. Thus, the value of C_{ij} ranged from 0 (nodes were never co-assigned to the same community) to 1 (nodes were always co-assigned to the same community). As with modularity maximization, we repeated this procedure for each participant and each value of γ separately.

2.2.6. Community co-assignment density

We compare detected communities with the system labels generated by Shen et al. (2013) by computing for each system its community co-assignment density and comparing that observed density against a chance model. Intuitively, co-assignment density measures the propensity for nodes of the same system to also be assigned to the same community and is derived from the elements of the co-assignment matrix, C_{ij}. Given a system, s, we can compute its co-assignment density as:

$$d_s = \sum_{ij \in s} C_{ij}$$

The value of d_s depends on the size of system s, and so we standardize (z-score) this value by comparing it against the density expected under a null model in which the number and size of communities stay the same but where nodes are otherwise randomly assigned to a community. Here, we report the standardized variant of co-assignment density.

2.2.7. Z-score rand index

Whereas the community co-assignment density compares individual partitions to individual systems, the Z-score Rand index compares entire partitions (Traud et al., 2011). Specifically, it extends the traditional Rand index, which measures the similarity of partitions X and Y, and analytically compares that value against what would be expected under a null model. The Rand index is expressed as a z-score with respect to that distribution with larger (positive) values indicating greater-than-expected levels of similarity between partitions X and Y.

2.2.8. Participation coefficient

In addition to co-assignment matrices, we also computed each node's participation coefficient (Guimera and Amaral, 2005). The participation coefficient of node i, which we denote as PC_i, ranges from 0 to 1 and indicates the extent to which node i's connections fall within a single community (values close to 0) or are evenly distributed (values close to 1) across communities (Fig. 1). Participation coefficients are calculated as:

$$PC_i = 1 - \sum_{s=1}^{K} (\kappa_{is}/k_i)^2$$

where κ_{is} is the total weight of connections node i makes to nodes in module s, and k_i is the total weight of all links incident on node i. Note that here we use an extension of the participation coefficient to signed networks. In this case, we report participation coefficients computed using only positive connections (an analogous participation coefficient can be computed using negative connections).

2.2.9. Permutation tests

Throughout this study we aggregate network measures at the level of individual nodes (brain areas) into canonical systems as defined by Shen et al. (2013). These include: default mode (DM), frontoparietal (FP), medial frontal (MF), medial temporal (MT), subcortical (SubC), visual association (VA), visual I (VI), and visual II (VII) systems. To assess system-level effects, we use a permutation-based statistical approach. For a given network measure, e.g. participation coefficient, we compute for each system the mean value across all nodes assigned to that system. Then we standardize (z-score) these mean values against a null distribution in which we randomly and uniformly permute system labels. In all cases, we repeat these permutations 10,000 times. The z-scored value for system s is calculated as:

$$z_s = (x_s - \mu_s)/\sigma_s$$

where x_s is the observed mean value of measure x and μ_s and σ_s are estimates of the mean and standard deviation obtained from the permutation tests. Z-scores were subsequently transformed into p-values. When appropriate, reported p-values were corrected for multiple comparisons by fixing the false discovery rate at $q = 0.05$ (Benjamini and Hochberg, 1995).

2.2.10. Analysis overview

Our analysis pipeline was as follows (Fig. 2): First, we used Pearson's correlations to estimate functional connectivity RS networks for each participant (Fig. 2a). Next, we used a data-driven approach to detect, for each participant, functional communities (Fig. 2b), and examine the functional connectivity magnitude of brain regions across their functional communities (Fig. 2c). We then computed for each participant their functional community co-assignment (Fig. 2d) and regional participation coefficients (Fig. 2e).

3. Results

3.1. Detected communities are variable across subjects but reflect canonical system-level organization

As a first step, we used modularity maximization to partition functional brain networks into communities— groups of nodes that are strongly connected to one another, but weakly connected between communities. Although the detected communities were variable, they nonetheless resembled the brain's known system-level organization (Power et al., 2011). Modularity maximization is a data-driven method for assigning a network's nodes to modules and detecting a network's modular structure. Modules are groups of nodes that are densely connected to one another and thought to support specialized information processing.

To demonstrate this, we used a multi-scale analog of modularity maximization to decompose participants' functional connectivity networks into communities (Fig. 3a). While we varied in our analysis the structural resolution parameter, γ, the association of network metrics at different resolutions with DT scores were highly correlated (SI Fig. 2). As such, all reported correlations represent averages across γ unless stated otherwise. We then compared these data driven identified communities to the Shen atlas (Shen et al., 2013) partition of neural systems (Fig. 3b). To do so, we first computed for each participant their community co-assignment matrix (how frequently are nodes u and v assigned to the same community, (Fig. 3c). Next, to demonstrate that these communities exhibited overlap with canonical brain systems, we computed two statistics: 1) the z-score of the Rand index and 2) normalized co-assignment density. The z-score of the Rand index (z-Rand) is a scalar whose value represents the similarity of two partitions to one another. Here, we compared detected partitions with the system partition derived in Shen

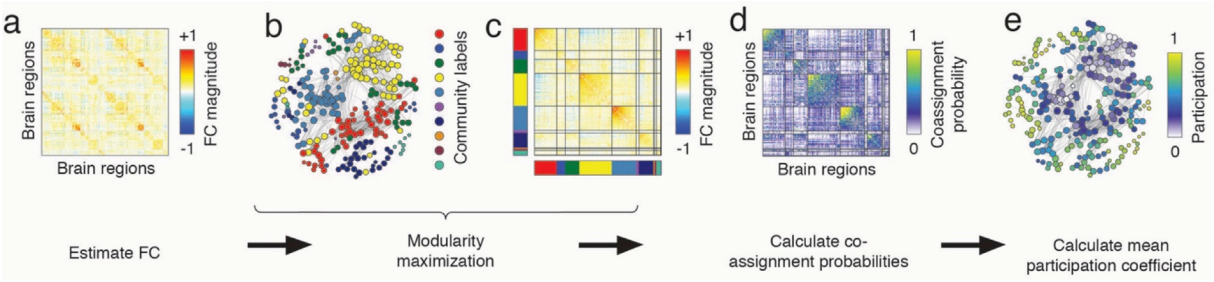

Fig. 2. Overall analysis flow of our study. (*a*) Our analysis began with functional connectivity matrices. We then subjected these matrices to a data-driven modularity maximization approach, which generated estimates of community structure. (*b*) We show here a force-directed layout of a typical network (thresholded at 7.5% for visualization) with communities by color. (*c*) The same network is shown in *1a* but with rows and columns ordered by detected communities. (*d*) We iterated the community detection approach many times, generating a series of potentially dissimilar community partition estimates. These were aggregated and used to construct a co-assignment matrix, whose elements equal to the fraction of partitions in which every pair of nodes were both assigned to the same community. (*e*) Given a modular partition, we also calculated each node's participation coefficient, which measured the extent to which its connections were uniformly distributed across communities.

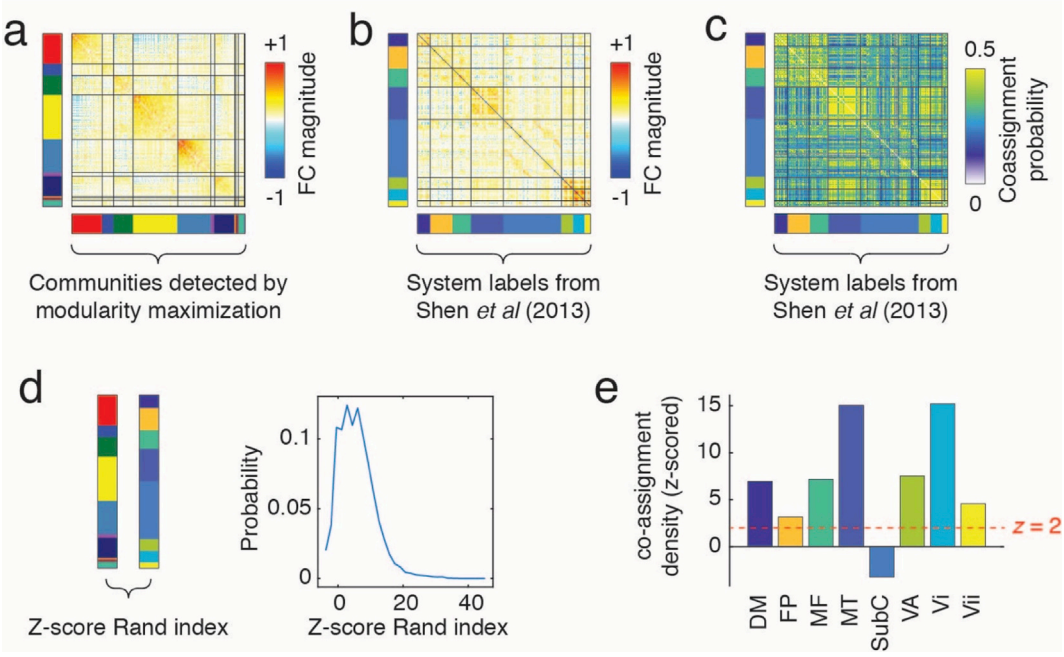

Fig. 3. Detecting functional communities across participants and comparing them to the Shen atlas system partition. (*a*) Functional connectivity matrix with rows and columns reordered by communities detected using modularity maximization. (*b*) Same matrix reordered by system labels from Shen et al. (2013). (*c*) Co-assignment matrix whose elements were estimated based on detected communities, but shown, here, reordered according to Shen et al. system labels. (*d*) We compared the detected communities with the Shen labels by computing the z-score of the Rand index. In general, larger values indicated greater similarity. (*e*) We calculated the z-scored co-assignment density for each Shen system, as the sum of all elements in the co-assignment matrix that fell within a given system. These values were then standardized against a permutation-based null model and expressed as z-scores.

et al. (2013). In general, larger values of *z*-Rand indicate greater similarity between detected communities and the canonical systems. The normalized co-assignment density, on the other hand, was computed at the level of individual brain systems and measures how frequently nodes in the same system were co-assigned to the same community by the modularity maximization algorithm. As with *z*-Rand, we standardized this measure (based on a permutation test) and express it as a *z*-score for each system.

In general, we found a strong correspondence between the detected communities and the systems derived by Shen et al. (2013). We found that the average *z*-Rand across all partitions (5.72, interquartile range of [1.68,8.79]) was greater than expected by chance ($p < 0.05$, permutation test), suggesting that at the level of whole-brain partitions, the detected communities exhibited a broad correspondence with known divisions of the brain into cognitive systems (Fig. 3d). Next, we generated a composite co-assignment matrix by averaging data from all participants and computed the co-assignment density within each of the eight systems in Shen et al. (2013). With the exception of the subcortical system, we found that each system exhibited co-assignment densities greater than chance ($p < 0.05$, permutation test; Fig. 3e).

To achieve this analysis, we used a data-driven approach to derive clusters (communities) of brain regions based on connectivity information alone. Importantly, we demonstrate that the detected communities correspond to known anatomical and functional subdivisions of the human brain. This comparison is carried out using the z-scored Rand index (Traud et al., 2011). Essentially, this measure estimates the degree of similarity between two sets of clusters while correcting for biases that might be introduced by the number and size of the clusters. Notably, while the relationship of the detected communities and the network labels from Shen et al. (2013) passes statistical tests of significance, it is

also inexact. While the origins of this inexactness are unclear, one possible explanation is that community structure, when evaluated at the level of individual participants, is variable and may not match system labels defined at the level of the group (e.g., Horien et al., 2019). In the rest of this paper, we investigate the relationship of this variability with an index of creativity.

3.2. Creative thinking ability is marked by differences in community structure

In the previous section we showed that, across a large cohort, functional brain networks can be partitioned into communities that recapitulated previously-described cognitive systems. We also demonstrated that these communities varied across individuals and repeated runs of the community detection algorithm. We hypothesized that this variance was related to inter-individual differences in creative ability, as measured by DT. To test this hypothesis, we first computed for each participant their community co-assignment matrix, whose elements measure, in a graded sense, the probability that two nodes were assigned to the same community. Then, using a mass-univariate testing procedure, we computed the correlation of community co-assignments with participants' DT scores.

In agreement with previous reports (Beaty et al., 2018), we found community-level correlates of creative thinking distributed across the entire brain and involving virtually all subsystems (Fig. 4a and b). To provide a more intuitive and visual summary of these findings, we calculated for each network node the mean correlation of its connections with DT indices. To further summarize these findings and at the system-level, we aggregated mean node-level correlations by system and computed the mean correlation over all constituent nodes. We then transformed each mean correlation value into a *z*-score by comparing it against the distribution of correlation values that are expected had communities been randomly and uniformly permuted (1000 permutations; Fig. 4c). We found that increases in DT scores were accompanied by a consolidation of medial temporal areas into the same community ($p < 0.05$, non-parametric permutation test; Fig. 4d). Furthermore, we also found a fragmentation of subcortical communities ($p < 0.05$, non-parametric permutation test; Fig. 4d). These within-system effects occurred in tandem with a series of between-system effects, which included increased co-assignment of medial frontal areas with visual, visual association, and medial temporal systems, as well as decreased co-assignment of subcortical systems with visual and fronto-parietal networks, and visual with visual association networks ($p < 0.05$, non-parametric test; Fig. 4c). Collectively, these findings posit a link between the brain's community-level functional architecture and an individual's DT scores (see Fig. 4e for an example).

3.3. Creative thinking ability is marked by redistribution of network hubs

Participation coefficient is a network measure defined at the level of individual nodes that indicates the extent to which a nodes' connections are distributed uniformly across modules (high participation) or concentrated within a module (low participation; Guimera and Amaral, 2005). Because high participation nodes connect to many different modules and because modules are thought to support specialized brain function, nodes with high participation are thought to participate in multiple functional domains.

While participation coefficient (PC) has been studied extensively in the context of functional brain networks (Bertolero et al., 2018; Gordon et al., 2018; Power et al., 2013), little is known about how PC and the spatial distribution of hubs reconfigure in higher-creative individuals relative to lower-creative individuals. To explore this question, we computed for each participant their PC for each of the 268 brain regions (Fig. 5a) and ranked these values. The ranking of the PC was done to remove inter-individual differences in baseline PC, which can be driven by global network properties (e.g. mean connection weight; See SI Fig. 3 for distribution of PC across the brain and across systems). Then we calculated for each brain region the correlation across all participants of ranked PC with their DT scores (Fig. 5c). Interestingly, we found considerable heterogeneity in terms of PC-creativity associations. In particular, we found that brain regions traditionally associated with the default mode network exhibited increased PC ($p < 0.05$, permutation test; Fig. 5b). That is, connections made by default mode areas are distributed across many communities in creative individuals, whereas those same areas tend to concentrate their connections within a few communities in the case of lower creativity individuals. Conversely, we found that brain regions in the medial temporal cortex exhibited significant decreases in PC ($p < 0.05$, permutation test; Fig. 5b), meaning that their connections became more concentrated within a few communities in creative individuals (see Fig. 5d for an example).

4. Discussion

Recent network neuroscience investigations of creative thinking have

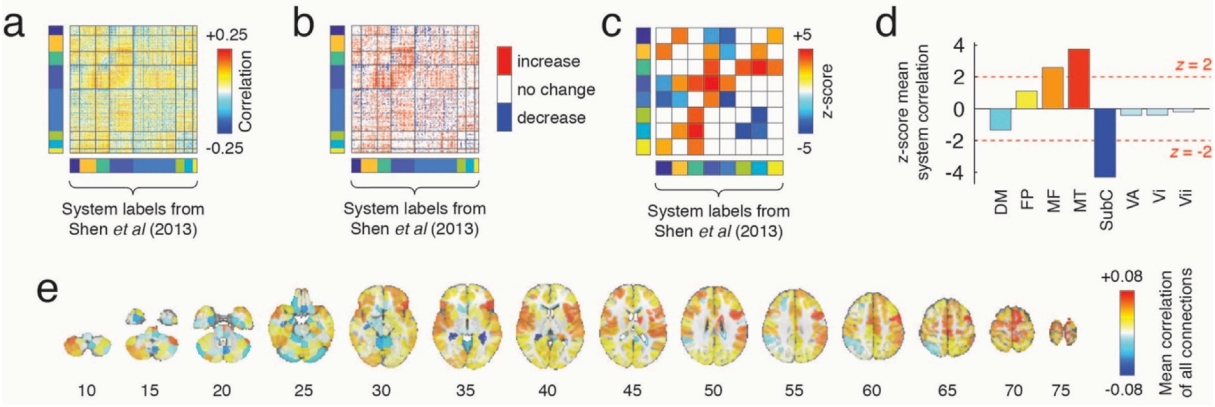

Fig. 4. Correlation of co-assignment probability and individual differences in creative ability. (*a*) Correlation magnitude of each functional connection's weight with creative ability across participants. (*b*) Same plot as in panel *a*; retaining only statistically significant correlations and showing only the sign of correlation (positive, negative, or not significant). (*c*) We aggregated the elements of the matrix shown in panel *a* by system labels reported by Shen et al. (2013) and compared the mean system-level correlations against the null distribution generated using a permutation-based null model. (*d*) For each node, we calculated its mean correlation with all other connections and subsequently aggregated these connections by system. As before, we compared these mean correlations against what would be expected had system labels been uniformly and randomly permuted. We expressed the original system-level values as z-scores relative to this distribution. (*e*) The mean correlation connectivity weight and creativity across all functional connections incident upon each node.

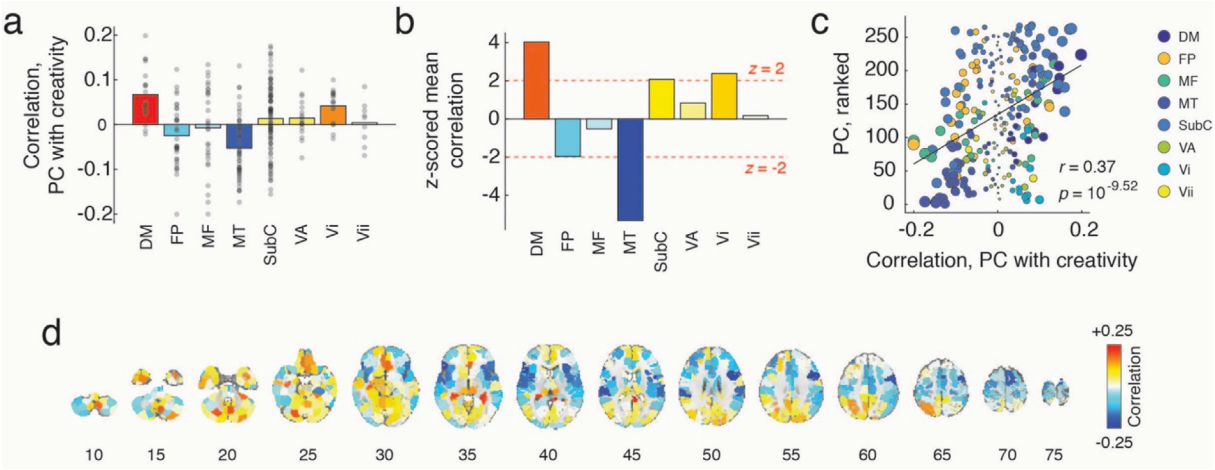

Fig. 5. Participation coefficients of functional brain communities and how they relate to individual differences in creativity. (*a*) Correlation coefficients of PC with creativity for every brain region grouped according to systems from Shen et al. (2013). (*b*) Correlation coefficients aggregated by brain system and standardized (z-scored) against a null distribution obtained by randomly and uniformly permuting system assignments. (*c*) Scatterplot of participant-averaged ranked PC against the correlation of PC with creativity. (*d*) Regional correlations of PC with creativity.

highlighted the significance of large-scale structural and functional brain connectivity patterns (Beaty et al., 2018; Beaty et al., 2019; Kenett et al., 2018). In the current study, we extend this line of inquiry by exploring how individual differences in creative thinking relate to meso-scale properties of RS functional brain networks. Specifically, we examined network science measures related to community structure—decompositions of a network into segregated clusters (communities) that are believed to reflect brain systems that support specialized information processing (Bertolero et al., 2015; Gallen and D'Esposito, 2019; Sporns and Betzel, 2016).

First, we show that, across participants, increases in creative thinking ability are accompanied by changes in community structure. Among the most salient is the consolidation of medial temporal areas into cohesive communities and the fragmentation of subcortical areas into smaller communities. A recent review examined the roles of the temporal lobes in the creative process, and proposed a theoretical framework highlighting the role of temporal regions in the creative process (Shen et al., 2017). According to this proposed model, creativity involves not only a cognitive control function that is realized by the ECN or an associative function that is realized by DMN, but also a 'temporal function' for integrating semantic information into novel associations and mental representations (Shen et al., 2017). Specifically, the authors argue that temporal regions play a role in the cognitive processing of insight through the formation of novel associations between concepts. Such a role is attributed to formation of representations (fusiform gyrus), semantic processing and inhibition of salient and prototypical responses (anterior and posterior MTG), and integrating and accessing semantic representations (anterior and posterior STG). Our findings for the role of a cohesive MT community in relation to DT scores supports this theoretical model of the temporal lobe in the creative process. Furthermore, we find a significant co-assignment relationship between the MT community and a frontal community that we speculate may reflect the interaction of the 'frontal function' with the 'temporal function' in the creative brain at rest.

A few direct and indirect studies have examined the role of subcortical regions in creative thinking. While much more research is required, these studies highlight the role of the dopaminergic system in divergent thinking (Faust-Socher et al., 2014; Mayseless et al., 2013; Schuler et al., 2019; Takeuchi et al., 2010; Tik et al., 2018). In our study, the sub-cortical community was the only community that showed reduced co-assignment density with the Shen atlas and negatively correlated with the latent DT score. It is important to note that brain parcellation atlases, such as the Shen atlas reliably parcellate cortical brain regions and are less reliable in subcortical regions (Gordon et al., 2014). For example, Ji et al. (2019) have shown that there are many functionally-defined nuclei and areas in the subcortex. Thus, grouping these multiple subcortex components together as one community may dilute data heterogeneity. Furthermore, more accurate parcellations of subcortical structures are possible with increased field strength. To accurately and sensitively parcellate sub-cortical areas, high resolution 7T fMRI scans are required (Schuler et al., 2019; Tik et al., 2018). Finally, a recent study highlighted the need for a universal taxonomy of functional brain network classification in network neuroscience (Uddin et al., 2019). The authors also call for conducting a similar approach in relation to subcortical regions. Taken together, while subcortical regions play a role in creative thinking, our results regarding the subcortical community should be interpreted with caution, due to noise and coarse parcellation.

Next, we examined whether these changes in community structure relate to changes in the distribution of network hubs (quantified using the participation coefficient). We find that as DT scores increase, the default mode network occupies an increasingly hub-like role with its connections more frequently spanning modular boundaries, whereas medial temporal areas—which form increasingly segregated and cohesive communities—exhibit decreased hubness. These findings indicate that, in addition to variation in community structure itself, inter-individual differences in creative capacity are accompanied by variation in node roles. Previous studies have highlighted the role of the DMN in the creative process (Beaty et al., 2016, 2019; Gonen-Yaacovi et al., 2013) and how creativity is related to task-based coupling between default, executive, and salience networks (Beaty et al., 2015). Thus, we interpret our findings as highlighting the role of the RS DMN system as a 'hub system', playing a critical role in coordinating integration of information across other communities which relates to higher levels of creativity. The lower average participation coefficient of the medial temporal system corresponds with our finding of the importance of its cohesiveness in relation to individual differences in creativity. Together, these findings further highlight the role of a 'temporal function' (Shen et al., 2017) in creativity and its expression in the resting brain.

Our study has a few potential limitations. One limitation is the use of the Shen atlas and its identified communities (Shen et al., 2013). Currently, there is an open discussion on the use of different brain atlases in parcellating MRI data, as well as the need to move towards individual based parcellation approaches (Arslan et al., 2018; Eickhoff et al., 2018; Uddin et al., 2019). However, the Shen atlas has been shown to be a reliable parcellation atlas (Eickhoff et al., 2018). Another limitation is that our findings are based on relatively short RS scans, raising the question of how findings may relate to DT performance in a task-based

context (Laumann et al., 2015). However, recently Shi et al. (2018) found that RS functional connectivity relates to task-based functional connectivity during DT task performance, consistent with the tight correspondence typically observed between resting-state and task-based brain networks (Cole et al., 2014).

Another limitation relates to the complexity of DT and the more basic cognitive processes that realize it, such as cognitive control, memory, and attention (Acar and Runco, 2019; Barbot et al., 2019; Benedek and Fink, 2019; Vartanian et al., 2019). Individual differences in DT could arise from various sources, such as IQ, age, or gender, as well as from variance in basic cognitive processes. To address this issue, further research exploring the brain's mesoscale features and how it relates to creative thinking is required. Such future research should include control tasks to highlight mesoscale features that uniquely relate to DT and not to general cognitive capacities (e.g., contrasting creativity with intelligence; Kenett et al., 2018), and conduct such analysis on task-based fMRI data to determine how such features may predict creative capacity (e.g., Beaty et al., 2018). In that sense, our current study is merely a first step at moving from studying the brain's functional connectivity patterns to studying the brain's higher-order community structure in relation to the creative process.

In conclusion, the current study expands current findings on neural functional connectivity patterns in creativity (Beaty et al., 2019), extending examinations of large-scale networks to study the roles of meso-scale functional communities and how these properties relate to individual differences in creativity. Our findings highlight a 'temporal function' in the creative process, supported by a cohesive medial temporal community, and further illustrate the 'hub' role of the DMN in the creative process. Thus, examining the functional community structure of the creative brain at rest sheds further light on the neural realization of this complex cognitive process.

Declaration of competing interest

The authors declare no competing interests.

Acknowledgements

This research was supported by grant RFP-15-12 from the Imagination Institute (www.imagination-institute.org), funded by the John Templeton Foundation. The opinions expressed in this publication are those of the authors and do not necessarily reflect the view of the Imagination Institute or the John Templeton Foundation.

Appendix A. Supplementary data

Supplementary data to this article can be found online at https://doi.org/10.1016/j.neuroimage.2020.116578.

References

Abraham, A., 2018. The Neuroscience of Creativity. Cambridge University Press, Cambridge, UK.
Acar, S., Runco, M.A., 2019. Divergent thinking: new methods, recent research, and extended theory. Psychol. Aesthet. Creativ. Arts 13 (2), 153–158.
Arslan, S., Ktena, S.I., Makropoulos, A., Robinson, E.C., Rueckert, D., Parisot, S., 2018. Human brain mapping: a systematic comparison of parcellation methods for the human cerebral cortex. Neuroimage 170, 5–30.
Barbot, B., Hass, R.W., Reiter-Palmon, R., 2019. Creativity assessment in psychological research:(Re) setting the standards. Psychol. Aesthet. Creativ. Arts 13 (2), 233.
Bazzi, M., Porter, M.A., Williams, S., McDonald, M., Fenn, D.J., Howison, S.D., 2016. Community detection in temporal multilayer networks, with an application to correlation networks. Multiscale Model. Simul. 14 (1), 1–41.
Beaty, R.E., Benedek, M., Kaufman, S.B., Silvia, P.J., 2015. Default and executive network coupling supports creative idea production. Sci. Rep. 5, 10964.
Beaty, R.E., Benedek, M., Silvia, P.J., Schacter, D.L., 2016. Creative cognition and brain network dynamics. Trends Cognit. Sci. 20 (2), 87–95.
Beaty, R.E., Benedek, M., Wilkins, R.W., Jauk, E., Fink, A., Silvia, P.J., Hodges, D.A., Koschutnig, K., Neubauer, A.C., 2014. Creativity and the default network: a functional connectivity analysis of the creative brain at rest. Neuropsychologia 64, 92–98, 0.
Beaty, R.E., Christensen, A.P., Benedek, M., Silvia, P.J., Schacter, D.L., 2017. Creative constraints: brain activity and network dynamics underlying semantic interference during idea production. Neuroimage 148, 189–196.
Beaty, R.E., Kenett, Y.N., Christensen, A.P., Rosenberg, M.D., Benedek, M., Chen, Q., Fink, A., Qiu, J., Kwapil, T.R., Kane, M.J., Silvia, P.J., 2018. Robust prediction of individual creative ability from brain functional connectivity. Proc. Natl. Acad. Sci. Unit. States Am. 115 (5), 1087–1092.
Beaty, R.E., Seli, P., Schacter, D.L., 2019. Network neuroscience of creative cognition: mapping cognitive mechanisms and individual differences in the creative brain. Curr. Opin. Behav. Sci. 27, 22–30.
Benedek, M., Christensen, A.P., Fink, A., Beaty, R.E., 2019. Creativity assessment in neuroscience research. Psychol. Aesthet. Creativ. Arts 13 (2), 218–226.
Benedek, M., Fink, A., 2019. Toward a neurocognitive framework of creative cognition: the role of memory, attention, and cognitive control. Curr. Opin. Behav. Sci. 27, I116–I122.
Benedek, M., Jauk, E., Beaty, R.E., Fink, A., Koschutnig, K., Neubauer, A.C., 2016. Brain mechanisms associated with internally directed attention and self-generated thought. Sci. Rep. 6, 22959.
Benedek, M., Jung, R., Vartanian, O., 2018. The neural bases of creativity and intelligence: common ground and differences. Neuropsychologia 118 (PA), 1–3.
Benjamini, Y., Hochberg, Y., 1995. Controlling the false discovery rate: a practical and powerful approach to multiple testing. J. Roy. Stat. Soc. B 57 (1), 289–300.
Bertolero, M.A., Yeo, B.T., D'Esposito, M., 2015. The modular and integrative functional architecture of the human brain. Proc. Natl. Acad. Sci. Unit. States Am. 112 (49), E6798–E6807.
Bertolero, M.A., Yeo, B.T.T., Bassett, D.S., D'Esposito, M., 2018. A mechanistic model of connector hubs, modularity and cognition. Nat. Hum. Behav. 2 (10), 765–777.
Betzel, R.F., Bassett, D.S., 2017. Multi-scale brain networks. Neuroimage 160, 73–83.
Betzel, R.F., Bertolero, M.A., Bassett, D.S., 2018. Non-assortative community structure in resting and task-evoked functional brain networks. bioRxiv, 355016.
Betzel, R.F., Bertolero, M.A., Gordon, E.M., Gratton, C., Dosenbach, N.U.F., Bassett, D.S., 2019. The community structure of functional brain networks exhibits scale-specific patterns of variability across individuals and time. NeuroImage 202, 115990.
Betzel, R.F., Medaglia, J.D., Papadopoulos, L., Baum, G.L., Gur, R., Gur, R., Roalf, D., Satterthwaite, T.D., Bassett, D.S., 2017. The modular organization of human anatomical brain networks: accounting for the cost of wiring. Netw. Neurosci. 1 (1), 42–68.
Blondel, V.D., Guillaume, J.-L., Lambiotte, R., Lefebvre, E., 2008. Fast unfolding of communities in large networks. J. Stat. Mech. Theor. Exp. 2008 (10), P10008.
Cole, M.W., Bassett, D.S., Power, J.D., Braver, T.S., Petersen, S.E., 2014. Intrinsic and task-evoked network architectures of the human brain. Neuron 83 (1), 238–251.
Crossley, N.A., Mechelli, A., Scott, J., Carletti, F., Fox, P.T., McGuire, P., Bullmore, E.T., 2014. The hubs of the human connectome are generally implicated in the anatomy of brain disorders. Brain 137 (8), 2382–2395.
de Haan, W., van der Flier, W.M., Koene, T., Smits, L.L., Scheltens, P., Stam, C.J., 2012. Disrupted modular brain dynamics reflect cognitive dysfunction in Alzheimer's disease. Neuroimage 59 (4), 3085–3093.
Eickhoff, S.B., Yeo, B.T.T., Genon, S., 2018. Imaging-based parcellations of the human brain. Nat. Rev. Neurosci. 19 (11), 672–686.
Faust-Socher, A., Kenett, Y.N., Cohen, O.S., Hassin-Baer, S., Inzelberg, R., 2014. Enhanced creative thinking under dopaminergic therapy in Parkinson's disease. Ann. Neurol. 75 (6), 935–942.
Fink, A., Benedek, M., Koschutnig, K., Papousek, I., Weiss, E.M., Bagga, D., Schöpf, V., 2018. Modulation of resting-state network connectivity by verbal divergent thinking training. Brain Cognit. 128, 1–6.
Finn, E.S., Shen, X., Scheinost, D., Rosenberg, M.D., Huang, J., Chun, M.M., Papademetris, X., Constable, R.T., 2015. Functional connectome fingerprinting: identifying individuals using patterns of brain connectivity. Nat. Neurosci. 18 (11), 1664–1671.
Fortunato, S., 2010. Community detection in graphs. Phys. Rep. 486 (3–5), 75–174.
Fox, M.D., Raichle, M.E., 2007. Spontaneous fluctuations in brain activity observed with functional magnetic resonance imaging. Nat. Rev. Neurosci. 8 (9), 700–711.
Gallen, C.L., D'Esposito, M., 2019. Brain modularity: a biomarker of intervention-related plasticity. Trends Cognit. Sci. 23 (4), 293–304.
Gao, Z., Zhang, D., Liang, A., Liang, B., Wang, Z., Cai, Y., Li, J., Gao, M., Liu, X., Chang, S., 2017. Exploring the associations between intrinsic brain connectivity and creative ability using functional connectivity strength and connectome analysis. Brain Connect. 7 (9), 590–601.
Gonen-Yaacovi, G., De Souza, L.C., Levy, R., Urbanski, M., Josse, G., Volle, E., 2013. Rostral and caudal prefrontal contribution to creativity: a meta-analysis of functional imaging data. Front. Hum. Neurosci. 7, 465.
Good, B.H., De Montjoye, Y.-A., Clauset, A., 2010. Performance of modularity maximization in practical contexts. Phys. Rev. 81 (4), 046106.
Gordon, E.M., Laumann, T.O., Adeyemo, B., Huckins, J.F., Kelley, W.M., Petersen, S.E., 2014. Generation and evaluation of a cortical area parcellation from resting-state correlations. Cerebr. Cortex 26 (1), 288–303.
Gordon, E.M., Lynch, C.J., Gratton, C., Laumann, T.O., Gilmore, A.W., Greene, D.J., Ortega, M., Nguyen, A.L., Schlaggar, B.L., Petersen, S.E., 2018. Three distinct sets of connector hubs integrate human brain function. Cell Rep. 24 (7), 1687–1695.
Green, A.E., Cohen, M.S., Raab, H.A., Yedibalian, C.G., Gray, J.R., 2015. Frontopolar activity and connectivity support dynamic conscious augmentation of creative state. Hum. Brain Mapp. 36 (3), 923–934.

Gu, S., Satterthwaite, T.D., Medaglia, J.D., Yang, M., Gur, R.E., Gur, R.C., Bassett, D.S., 2015. Emergence of system roles in normative neurodevelopment. Proc. Natl. Acad. Sci. Unit. States Am. 112 (44), 13681–13686.
Guimera, R., Amaral, L.A.N., 2005. Functional cartography of complex metabolic networks. Nature 433 (7028), 895–900.
Hass, R.W., Rivera, M., Silvia, P.J., 2018. On the dependability and feasibility of layperson ratings of divergent thinking. Front. Psychol. 9 (1343).
Horien, C., Shen, X., Scheinost, D., Constable, R.T., 2019. The individual functional connectome is unique and stable over months to years. Neuroimage 189, 676–687.
Ji, J.L., Spronk, M., Kulkarni, K., Repovš, G., Anticevic, A., Cole, M.W., 2019. Mapping the human brain's cortical-subcortical functional network organization. Neuroimage 185, 35–57.
Jutla, I.S., Jeub, L.G.S., Mucha, P.J., 2011. A generalized Louvain method for community detection implemented in MATLAB. URL. http://netwiki.amath.unc.edu/GenLouvain.
Kenett, Y.N., Medaglia, J.D., Beaty, R.E., Chen, Q., Betzel, R.F., Thompson-Schill, S.L., Qiu, J., 2018. Driving the brain towards creativity and intelligence: a network control theory analysis. Neuropsychologia 118, 79–90.
Kline, R.B., 2015. Principles and Practice of Structural Equation Modeling. Guilford publications, New York, NY.
Latora, V., Marchiori, M., 2001. Efficient behavior of small-world networks. Phys. Rev. Lett. 87 (19), 198701.
Laumann, Timothy O., Gordon, Evan M., Adeyemo, B., Snyder, Abraham Z., Joo, Sung J., Chen, M.-Y., Gilmore, Adrian W., McDermott, Kathleen B., Nelson, Steven M., Dosenbach, Nico U.F., Schlaggar, Bradley L., Mumford, Jeanette A., Poldrack, Russell A., Petersen, Steven E., 2015. Functional system and areal organization of a highly sampled individual human brain. Neuron 87 (3), 657–670.
Li, J., Zhang, D., Liang, A., Liang, B., Wang, Z., Cai, Y., Gao, M., Gao, Z., Chang, S., Jiao, B., 2017. High transition frequencies of dynamic functional connectivity states in the creative brain. Sci. Rep. 7, 46072.
Mayseless, N., Uzefovsky, F., Shalev, I., Ebstein, R.P., Shamay-Tsoory, S.G., 2013. The association between creativity and 7R polymorphism in the dopamine receptor D4 gene (DRD4). Front. Hum. Neurosci. 7, 502.
Medaglia, J.D., Lynall, M.-E., Bassett, D.S., 2015. Cognitive network neuroscience. J. Cognit. Neurosci. 27 (8), 1471–1491.
Meunier, D., Lambiotte, R., Bullmore, E.T., 2010. Modular and hierarchically modular organization of brain networks. Front. Neurosci. 4, 200.
Muthén, L.K., Muthén, B.O., 2012. Mplus: statistical Analysis with Latent Variables, User's Guide. Muthén & Muthén, Los Angeles, CA.
Newman, M.E.J., Girvan, M., 2004. Finding and evaluating community structure in networks. Phys. Rev. E 69 (2), 026113.
Power, Jonathan D., Cohen, Alexander L., Nelson, Steven M., Wig, Gagan S., Barnes, Kelly A., Church, Jessica A., Vogel, Alecia C., Laumann, Timothy O., Miezin, Fran M., Schlaggar, Bradley L., Petersen, Steven E., 2011. Functional network organization of the human brain. Neuron 72 (4), 665–678.
Power, J.D., Schlaggar, B.L., Lessov-Schlaggar, C.N., Petersen, S.E., 2013. Evidence for hubs in human functional brain networks. Neuron 79 (4), 798–813.
Reichardt, J., Bornholdt, S., 2006. Statistical mechanics of community detection. Phys. Rev. 74 (1), 016110.
Rosenberg, M.D., Finn, E.S., Scheinost, D., Papademetris, X., Shen, X., Constable, R.T., Chun, M.M., 2016. A neuromarker of sustained attention from whole-brain functional connectivity. Nat. Neurosci. 19 (1), 165–171.
Rubinov, M., Sporns, O., 2011. Weight-conserving characterization of complex functional brain networks. Neuroimage 56 (4), 2068–2079.
Runco, M.A., Acar, S., 2012. Divergent thinking as an indicator of creative potential. Creativ. Res. J. 24 (1), 66–75.
Ryman, S.G., van den Heuvel, M.P., Yeo, R.A., Caprihan, A., Carrasco, J., Vakhtin, A.A., Flores, R.A., Wertz, C., Jung, R.E., 2014. Sex differences in the relationship between white matter connectivity and creativity. Neuroimage 101, 380–389.
Schuler, A.-L., Tik, M., Sladky, R., Luft, C.D.B., Hoffmann, A., Woletz, M., Zioga, I., Bhattacharya, J., Windischberger, C., 2019. Modulations in resting state networks of subcortical structures linked to creativity. Neuroimage 195, 311–319. https://doi.org/10.1016/j.neuroimage.2019.03.017.
Shen, W., Yuan, Y., Liu, C., Luo, J., 2017. The roles of the temporal lobe in creative insight: an integrated review. Think. Reas. 23 (4), 321–375.
Shen, X., Tokoglu, F., Papademetris, X., Constable, R.T., 2013. Groupwise whole-brain parcellation from resting-state fMRI data for network node identification. Neuroimage 82, 403–415.
Shi, L., Sun, J., Xia, Y., Ren, Z., Chen, Q., Wei, D., Yang, W., Qiu, J., 2018. Large-scale brain network connectivity underlying creativity in resting-state and task fMRI: cooperation between default network and frontal-parietal network. Biol. Psychol. 135, 102–111.
Silvia, P.J., Winterstein, B.P., Willse, J.T., Barona, C.M., Cram, J.T., Hess, K.I., Martinez, J.L., Richard, C.A., 2008. Assessing creativity with divergent thinking tasks: exploring the reliability and validity of new subjective scoring methods. Psychol. Aesthet. Creativ. Arts 2 (2), 68–85.
Sporns, O., Betzel, R.F., 2016. Modular brain networks. Annu. Rev. Psychol. 67 (1), 613–640.
Sun, J., Liu, Z., Rolls, E.T., Chen, Q., Yao, Y., Yang, W., Wei, D., Zhang, Q., Zhang, J., Feng, J., 2019. Verbal creativity correlates with the temporal variability of brain networks during the resting state. Cerebr. Cortex 29 (3), 1047–1058.
Takeuchi, H., Taki, Y., Hashizume, H., Sassa, Y., Nagase, T., Nouchi, R., Kawashima, R., 2012. The association between resting functional connectivity and creativity. Cerebr. Cortex 22 (12), 2921–2929.
Takeuchi, H., Taki, Y., Nouchi, R., Yokoyama, R., Kotozaki, Y., Nakagawa, S., Sekiguchi, A., Iizuka, K., Yamamoto, Y., Hanawa, S., 2017. Regional homogeneity, resting-state functional connectivity and amplitude of low frequency fluctuation associated with creativity measured by divergent thinking in a sex-specific manner. Neuroimage 152, 258–269.
Takeuchi, H., Taki, Y., Sassa, Y., Hashizume, H., Sekiguchi, A., Fukushima, A., Kawashima, R., 2010. Regional gray matter volume of dopaminergic system associate with creativity: evidence from voxel-based morphometry. Neuroimage 51 (2), 578–585.
Tik, M., Sladky, R., Luft, C.D.B., Willinger, D., Hoffmann, A., Banissy, M.J., Bhattacharya, J., Windischberger, C., 2018. Ultra-high-field fMRI insights on insight: neural correlates of the Aha!-moment. Hum. Brain Mapp. 39 (8), 3241–3252.
Traud, A.L., Kelsic, E.D., Mucha, P.J., Porter, M.A., 2011. Comparing community structure to characteristics in online collegiate social networks. SIAM Rev. 53 (3), 526–543.
Uddin, L.Q., Yeo, B.T.T., Spreng, R.N., 2019. Towards a universal taxonomy of macro-scale functional human brain networks. Brain Topogr. 32, 926–942.
van den Heuvel, M.P., Sporns, O., 2013. Network hubs in the human brain. Trends Cognit. Sci. 17 (12), 683–696.
Vartanian, O., Beatty, E.L., Smith, I., Blackler, K., Lam, Q., Forbes, S., 2018. One-way traffic: the inferior frontal gyrus controls brain activation in the middle temporal gyrus and inferior parietal lobule during divergent thinking. Neuropsychologia 118, 68–78.
Vartanian, O., Beatty, E.L., Smith, I., Forbes, S., Rice, E., Crocker, J., 2019. Measurement matters: the relationship between methods of scoring the Alternate Uses Task and brain activation. Curr. Opin. Behav. Sci. 27, 109–115.
Wei, D., Yang, J., Li, W., Wang, K., Zhang, Q., Qiu, J., 2014. Increased resting functional connectivity of the medial prefrontal cortex in creativity by means of cognitive stimulation. Cortex 51, 92–102.
Whitfield-Gabrieli, S., Nieto-Castanon, A., 2012. Conn: a functional connectivity toolbox for correlated and anticorrelated brain networks. Brain Connect. 2 (3), 125–141.
Zhu, W., Chen, Q., Xia, L., Beaty, R.E., Yang, W., Tian, F., Sun, J., Cao, G., Zhang, Q., Chen, X., Qiu, J., 2017. Common and distinct brain networks underlying verbal and visual creativity. Hum. Brain Mapp. 38 (4), 2094–2111.